

# Design and Testing of a Multimode and In-Situ Propellant Feed System

IEPC-2024-302

*Presented at the 38th International Electric Propulsion Conference  
Pierre Baudis Convention Center • Toulouse, France  
June 23-28, 2024*

William P. Brabston<sup>1</sup>, Luke A. Marino<sup>2</sup>, Dan Lev<sup>3</sup>, and Mitchell L. R. Walker<sup>4</sup>  
*Georgia Institute of Technology, Atlanta, GA, 30332, USA*

**The Multimode/In-Situ propellant (MIST) system is designed to serve as a test bed to supply various alternative propellants for ground-based electric propulsion applications. The MIST system can operate in multiple modes and supply gas mixtures, such as air, condensable vapors, such as water vapor, and pure gases, such as xenon, at a designed mass flow rate range of 0.5 to 10 mg/s in all modes. The MIST system design process involves implementing a system engineering design approach with high-level system requirements, a risk analysis, and a configuration sweep using a figure of merit approach. The system requirements are then validated using leak, condensation, and 5-kW Hall effect thruster hot-fire validation tests. With the currently installed components, the MIST system can supply pure gases with a flow rate uncertainty of  $\pm 1\%$ , gas mixtures with a composition and flow rate uncertainty of  $\pm 1.4\%$ , and condensable gases with a flow rate uncertainty of  $\pm 0.56\%$ .**

## I. Introduction

MULTIMODE and in-situ propellants and propulsion systems have garnered recent interest for use in electric propulsion (EP) devices. Multimode propulsion systems consist of two separate propulsion architectures that are integrated on a common spacecraft platform and can share a common propellant. The two propulsion devices, often chemical and electric, allow for a spacecraft to operate in either a high-efficiency or high-thrust mode without the additional cost, weight, and complexity of two entirely independent propulsion systems<sup>1-3</sup>. In-situ propellants, on the other hand, are propellants that are harvested in space, either in orbit or on various planetary bodies. In-situ propellants are useful in that the propellant can be harvested and resupplied away from Earth, which allows spacecraft to carry less propellant on the initial launch and extend their operational lifetime in space<sup>4</sup>.

There are multiple arrangements of thruster and propellant combinations that can be used for multimode and in-situ systems, but one of the common propellants that has gained attention in recent years across both areas is water<sup>5-7</sup>. Water is beneficial in that an electrolysis process can separate it into hydrogen and oxygen constituents, which are prominent fuels for bi-propellant chemical propulsion systems in high-thrust multimode applications<sup>6</sup>. Furthermore, water stores at a relatively high density compared to other gaseous propellants and maintains a high specific impulse due to its low particle mass, which are both beneficial for a high-efficiency, EP multimode application<sup>7</sup>. Water is also found on a myriad of planetary bodies in the universe<sup>8</sup>, making it ideal for in-situ propellant harvesting on deep space missions.

Many EP devices, such as Hall effect thrusters (HETs), rely on gaseous products to operate, but at room temperatures and pressures, water will condense. Along with condensability risks, water in its liquid state maintains a relatively high surface tension compared to other condensable liquids due to its intermolecular hydrogen bonding<sup>9</sup>.

---

<sup>1</sup> Graduate Student, School of Aerospace Engineering, wbrabston3@gatech.edu

<sup>2</sup> Graduate Student, School of Aerospace Engineering, lukemarinno54@gatech.edu

<sup>3</sup> Research Engineer, School of Aerospace Engineering, dan.lev@gatech.edu

<sup>4</sup> Professor and School Chair, School of Aerospace Engineering, mitchell.walker@ae.gatech.edu

These characteristics of water pose challenges to developing and operating a propellant feed system for EP ground testing, especially in maintaining steady flow over time.

Another common in-situ propellant is air, which can be harvested for satellite propulsion in very low Earth orbit (VLEO), which is generally defined as orbits less than 450 km. Harvesting air in VLEO could provide an indefinite supply of propellant, which would greatly extend the lifetime of satellites in this orbit<sup>10</sup>. VLEO is an attractive orbit due to its close positioning to Earth, offering better latency of communication systems and higher resolution ground imaging along with numerous other benefits<sup>11,12</sup>. The VLEO environment is complex, where the atmospheric composition changes as a function of altitude, time of day, time of year, and solar activity<sup>13,14</sup>. These factors can cause the input propellant composition to consistently change in a VLEO in-situ electric propellant thruster, resulting in varying performances and efficiencies.

To facilitate ground testing and capture the capabilities and performances of water, air, and other multimode and in-situ propellants in an EP device, namely a HET, the authors designed a propellant feed system that can produce and deliver these various products. This paper overviews the design, calibration, and verification of this novel propellant feed system, while placing special attention on the numerous risks and constraints imposed by the various propellant constituents. This propellant feed system can operate in a pure gas, pure gas mixture, condensable product, or condensable product/pure gas mixture operating mode, thus serving as a testbed for various alternative propellants in EP devices. To verify the design and operation of this feed system, the authors tested the delivery of xenon, nitrogen, a krypton/argon mixture, and water vapor in a hot-fire test with a 5-kW P5 HET.

## II. Design Space Requirements and Configuration Selection

The design of the Multimode/In-Situ propellant (MIST) system followed the recommended practices laid out in the NASA Systems Engineering Handbook for system design<sup>15</sup>. The first subsection presents design decisions enacted from the high-level system requirements and risks considered in the design of the MIST system. The next subsection presents a configuration survey of potential methods to meter the water constituent and then selects the winning configuration using a figure of merit approach.

### A. High-Level System Requirements

The design of the MIST system was based on a set of high-level design requirements that highlight how the system should operate. The overall design intent of the MIST system is to serve as a testbed for various alternative propellants used in an EP capacity. Specifically, the MIST system is designed to operate on water vapor and a mix of gaseous propellants, such as air; however, this use case can be expanded to include other condensable propellants and gaseous mixtures as the field of alternative propellants continues to evolve.

The primary EP device considered in the MIST system design is a HET, which dictates some of the MIST design requirements, such as the requirement to supply propellants in a vapor form and the required mass flow rate range in the order of 1-10 mg/s. The other system requirements are derived with ease of use, calibration capability, safety, and material compatibility in mind and influenced by the NASA Preferred Practices Design Considerations for Fluid Tubing Systems document (NASA PD-ED-1224)<sup>16</sup>. The list of high-level MIST system design requirements is presented in Table 1.

**Table 1. MIST system high-level requirements.**

#	Requirement Description
1	MIST system <u>shall</u> operate with pure gas, water vapor, and gaseous mixture constituents
2	MIST system <u>shall</u> supply all products in a gaseous form
3	MIST system <u>shall</u> supply a gas, independent from the anode and non-corrosive, to the cathode
4	MIST system <u>shall</u> supply constituents in a mass flow rate range of 0.5-10 mg/s
5	MIST system <u>shall</u> supply constituents with a maximum mean flow rate uncertainty of $\pm 5\%$ of the operational setpoint
6	MIST system <u>shall</u> supply a steady mass flow rate of constituents with a maximum peak-to-peak oscillation of $\pm 10\%$ of the flow rate setpoint
7	MIST system <u>shall</u> not exhibit a propellant leak greater than 0.5 sccm on nitrogen at 30 psi
8	MIST system <u>shall</u> not pose a significant safety risk for operators
9	MIST system <u>shall</u> be constructed of materials compatible with water and oxygen

Operation with alternative propellants can introduce some inherent risks, both to user safety and in meeting the required design intent of the propellant feed system. These feed system risks are outlined in Table 2, and are used to influence design decisions for the MIST system to mitigate these risks as much as possible. In this table, the risks are also classified by their severity, which can rank as high, medium, or low. A high severity risk requires significant design considerations to mitigate that risk and is addressed first as it can require significant modifications to the overall feed system architecture. A medium severity risk requires moderate design modifications to reduce that risk and is addressed next as it generally involves adding several additional components to the propellant feed system. Finally, a low-severity risk requires minor modifications to mitigate that risk and generally only involves adding minor components to the feed system that do not affect the overall feed system design.

**Table 2. MIST system risk analysis.**

#	Risk Description	Severity
i	Water is condensable at standard pressures and temperatures	High
ii	Liquid water has high surface tension causing potentially unsteady flow rate control	Medium
iii	Oxygen can cause flammability risks	Low
iv	Oxygen and water can cause corrosive risks	Medium
v	Water vaporization can cause high temperatures and pressures	Low

The high-level design requirements and risks define the design space for the MIST system. Within this design space, numerous design decisions were made to meet the system requirements and mitigate the risks. Table 3 presents these design decisions along with the respective requirements and risks upon which that design decision is based, where many of the design decisions are made to address the condensability risk of the water constituent as this risk is high severity. These design features direct the overall configuration and design of the MIST system.

**Table 3. Requirement and risk-based design decisions.**

#	Requirement Basis	Risk Basis	Design Description
1a	1	i	Metering of the water and gaseous constituents will be separate.
2a	2	i	The MIST system will possess a heating system for water vaporization.
2b	2	i	Installed pressure transducers and thermocouples will verify water vapor remains in a vapor state.
3a	3	~	The MIST system will have an independent flow path to run the cathode on xenon or krypton.
4a	4	~	All installed flow devices will be rated for the mass flow rate range of 0.5-10 mg/s.
5a	5	~	All constituents will have an independent calibration method to validate flow rate uncertainty.
5b	5	i	The MIST system will possess an additional calibration method to ensure water vapor does not condense.
6a	6	ii	The MIST system will contain a plenum to mitigate water flow rate oscillations.
6b	6	~	The MIST system will have the capability to record the flow rate of all constituents in real time.
7a	7	~	A leak check procedure will be implemented to verify the leak rate requirement.
8a	8	iii	Oxygen operation will require an installed oxygen flame arrestor.
8b	8	v	All heated lines will have insulation to reduce burn risks from high temperatures.
8c	8	v	The MIST system will have a relief valve to maintain safe working pressures.
9a	9	iii	All oxygen-wetted surfaces will be maintained at a temperature significantly below metal ignition temperatures.
9b	9	iv	All water and oxygen-wetted surfaces will be constructed with stainless steel.

## B. Water Metering Configuration Survey

As seen in Table 3 design decision 1a, the water constituent is independently supplied and metered from the rest of the gas constituents due to the complexities in metering low flow rates of water and its condensability risk. There are different methods to meter water, each with distinct advantages and disadvantages. Three potential methods are displayed in Fig. 1, including pressurant-driven flow control, steam flow control, and liquid water flow control. In the diagram below, MFC indicates the mass flow controller.

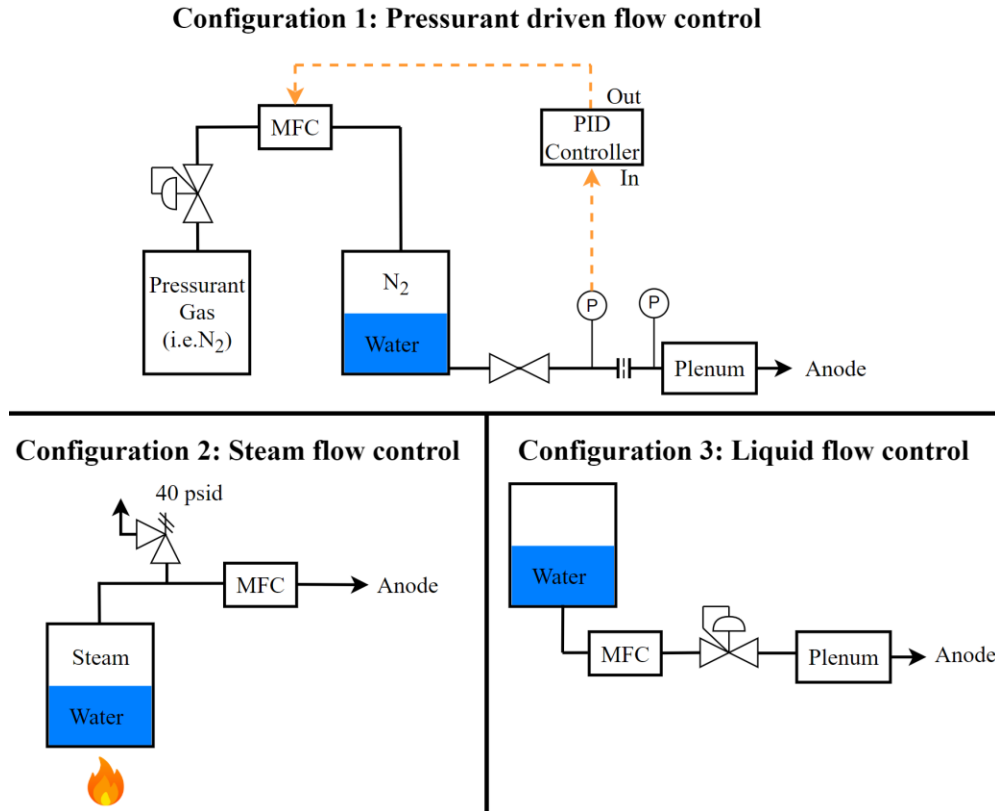


Figure 1. Water metering configuration survey.

Pressurant-driven flow control describes the process where an inert pressurant gas, typically nitrogen, drives water across a restrictive orifice plate by varying the head pressure of the water. For an orifice with a fixed liquid impedance, temperature, and backpressure, the water flow rate across that orifice is a direct function of upstream pressure, as referenced in ISO 5167<sup>17</sup>. The pressure is recorded using an upstream pressure transducer, and the signal is fed to a PID controller, which controls the pressure via an MFC. A major challenge that exists with this method is that the orifice area needs to be extremely small to regulate a low flow rate of water. With a small cross-sectional orifice area and the high surface tension of water, the pressurant pressure could become prohibitively high for the upper mass flow rate range.

Steam flow control is an alternative water flow control method where water is boiled in a reservoir to increase the pressure of the steam upstream of an MFC. Most MFCs require a pressure differential across them to operate so that the steam would provide the necessary pressure differential. Shirasu *et al.*<sup>7</sup> and Nakagawa *et al.*<sup>18</sup> have demonstrated a steam control flow system, using bang bang valve control, for use on a HET and electron cyclotron resonance thruster, respectively. Gallucci *et al.* have also designed a steam flow control system for use on their microwave electrothermal thruster, but has not published specifics on the steam MFC configuration<sup>19</sup>. Some challenges that arise with this method are that many MFCs are not compatible with the high temperature required for steam control and the time required to vaporize water can make it difficult to quickly change flow rates or maintain a constant upstream pressure.

Finally, liquid water flow control maintains the water flow rate using a liquid-based MFC. To isolate the liquid MFC from vacuum, a flow restrictor, such as a backpressure regular (shown in Fig. 1) or capillary tube is required downstream of the MFC. Tejada *et al.* demonstrated liquid flow control for a water vapor HET application using a

capillary as a flow restrictor<sup>5</sup>. A major challenge that arises in liquid flow control is that there are a limited number of liquid MFCs that exist for the required flow rate range.

The authors selected the water control method using a figure of merit approach applied to each of the configurations and judged based on how well they fit criteria derived from the high-level system requirements. The selected criteria are cost, complexity, flow steadiness, total flow uncertainty, user safety, and material compatibility, and each criterion is equally weighted. The configurations are qualitatively ranked in each criterion, with 1 being the best and 3 being the worst, and the scores are summed for each configuration. The figure of merit analysis is shown in Table 4.

**Table 4. Water metering configuration figure of merit selection.**

Configuration	Cost	Complexity	Flow Steadiness	Flow Uncertainty	Safety	Material Compatibility	Total
Pressurant Driven	1	2	3	3	2	1	12
Steam Control	3	3	2	2	3	3	16
Liquid Control	2	1	1	1	1	2	8

The winning configuration from the figure of merit approach is liquid flow control, primarily due to the simplicity of the design. This configuration also allows for the most direct control over the water flow rate. Within liquid flow control, various flow controller types are available, including Coriolis, thermal-based, micro pump-fed, and syringe pump. The authors selected to use a syringe pump configuration due to the relatively low cost, high flow rate range, and high accuracy these pumps allow.

A syringe pump operates by using a high-precision linear stepper motor to compress the plunger of a gas-tight syringe pre-loaded with deionized water. The speed of the linear stepper motor and the diameter of the syringes dictate the resultant water flow rate. Syringe pumps are heavily used in the medical industry for precise intravenous liquid drug delivery<sup>20,21</sup>. Due to the adaptability of operating with different syringe diameters and linear pusher speeds, syringe pumps can operate with flow rate ranges anywhere from  $\mu\text{L/hr}$  to  $\text{mL/s}$  with less than 1% uncertainty. These pumps also excel with viscous liquids and liquids with a high surface tension, making them ideal for the MIST system application.

### III. Propellant Feed System Design Overview

This section overviews the final design of the MIST system. The first subsection presents the process and instrumentation diagram for the MIST system, and the subsequent subsections discuss the operation of the MIST system in pure gas, gas mixture, and water vapor modes. The final subsection presents the control method, user interface, and data acquisition method for the MIST system.

#### A. Process and Instrumentation Diagram of Final Design

Fig. 2 presents the final process and instrumentation diagram (P&ID) of the MIST system. The flow paths for each operational mode are highlighted to distinguish the unique hardware and devices used in each mode. The requisite hardware derived from the requirement and risk-based design decisions in Table 3 have been included in the P&ID.

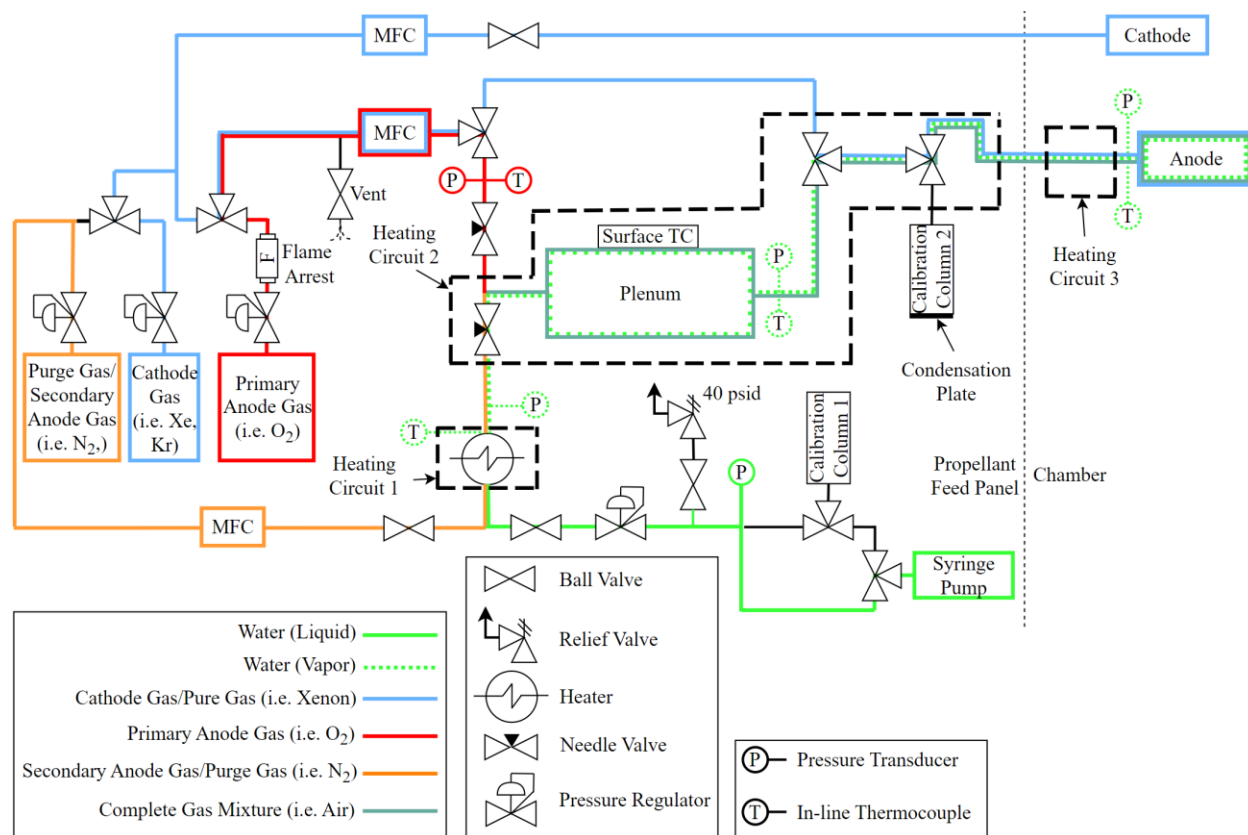


**Figure 2. MIST system process and instrumentation diagram. The colors represent flow paths in the various operating modes.**

### B. Pure Gas Operation

The first operational mode of the MIST system is the pure gas mode, which consists of a single, non-condensable gas supplied to the anode and cathode. The gas can be shared between the anode and cathode (such as xenon supplied to both) or can be distinct gases between the two (such as nitrogen to the anode and xenon to the cathode). The shared gas flow path is shown in light blue in the Fig. 2 P&ID, where the anode path utilizes a plenum bypass line for simplicity. MKS GE50A MFCs meter both the anode and cathode lines, and their operational flow rates are independently calibrated with a MesaLabs DryCal 800 in accordance with the recommended practice outlined in Snyder *et al.*<sup>22</sup>. The MFCs have a resultant uncertainty of 1% of the flow rate setpoint, leading to a maximum test uncertainty of  $\pm 0.10$  mg/s at a 10 mg/s setpoint flow rate.

### C. Gas Mixture Operation

The next operational mode of the MIST system is the gas mixture mode, which consists of supplying a variable mixture of two non-condensable gases to the anode, such as an air mixture. The cathode can operate either using one of the gases in the mixture or by using a third, independent gas. For gas mixtures containing oxygen, an oxygen flame arrest is installed on the primary anode gas line to prevent flame propagation given an ignition event. The secondary anode gas is metered using an additional MKS GE50A MFC, and the two gases mix in a 0.5L stainless steel plenum. Needle valves installed upstream of the plenum impose a pressure gradient to prevent the gases from backstreaming into the opposing fluid path. The complete gas mixture then flows out of the plenum and continues to the thruster anode. Since both anode gases are actively controlled using MFCs, the mixture ratio can be changed throughout the course of a test, simulating various atmospheric conditions in a VLEO environment.

The third MFC is also independently calibrated with a MesaLabs DryCal 800. The mixture composition is not directly measured; however, pressure transducers upstream of both needle valves ensure steady flow from both gas constituents. If the flow of each constituent is steady, seen with a steady pressure measurement, constituent backstreaming is mitigated, and there are no mass loss mechanisms, the final mixture composition will remain constant in the gas mixture. The gas mixture operation mode presents a flow rate and composition uncertainty of 1.4% of the flow rate setpoint, leading to a maximum test uncertainty of  $\pm 0.14$  mg/s at a 10 mg/s setpoint flow rate.

#### **D. Water Vapor Operation**

Another operational mode of the MIST system is the water vapor mode, which consists of supplying water vapor to the anode and an independent, non-condensable gas to the cathode. The deionized water propellant is metered in liquid form using a Cole Parmer six-channel syringe pump operating with KD Scientific 50 mL stainless steel gas-tight syringes. Pressure is held on the syringe pump using an Equilibar ZF1SNN8 backpressure regulator at a set pressure of 30 psig. Upstream of the backpressure regulator is held liquid-locked with water, which can cause rampant increases in pressure with the actuation of the syringe pump. To mitigate pressure spikes, a 40 psid relief valve is installed in the liquid-locked region, where an air pocket is held between the ball valve and the relief valve. The air allows for a quick release of pressure and acts as a spring to slow the rate of pressure rise. The pressure will rise in the liquid-locked section until it reaches 30 psig, verified by an installed pressure transducer, at which point the water will pass through the backpressure regulator at a rate equal to the supply rate of the syringe pump.

Once the water exits the backpressure regulator, it passes through a Watlow Fluent FLC-2 in-line heater, which is a device that forces the water over a series of heated baffles to vaporize the liquid water. The water is maintained in a vapor state for the remainder of the feed system until it reaches the thruster anode. The vaporization process creates some pressure oscillations, which are damped as the water vapor passes through the 0.5L plenum. To ensure the water vapor does not condense, the remainder of the propellant lines after the in-line heater are coated in a thermal transfer compound, wrapped in heater wire, and insulated using fiberglass and alumina insulation. A control system maintains the in-line heater and heated lines at a constant, set temperature. A series of pressure transducers and in-line thermocouples throughout the remainder of the heated section ensures the water remains in a vapor state. The pressure transducers in the vapor region serve an additional function of acting as live flow rate monitors. Since the thruster anode has a fixed cross-sectional area and the water vapor is maintained at a constant temperature, the water vapor flow rate into the anode is directly a function of the upstream pressure. If this pressure is constant, and the water is not condensing anywhere, the vapor flow rate into the anode is equal to the commanded flow rate from the syringe pump. Once testing is complete, a dry purge gas is flowed through the water vapor section of the MIST system to purge any remaining condensable vapors.

Prior to flowing water vapor to the thruster, the MIST system undergoes a rigorous calibration process to ensure the syringe pump is outputting the correct flow rate and the water vapor is not condensing in the system. The syringe pump flow rate is calibrated using a 100 mL Koflo calibration column, denoted as calibration column 1 in Fig. 2. Calibration column 2 is then used to ensure the water vapor does not condense in the feed system. This calibration column is positioned just before the vacuum chamber propellant feedthrough, and after the highest-pressure region in the MIST system. The tubing just before calibration column 2 is equipped with a water chiller sleeve and the bottom of calibration column 2 is fitted with a stack of six Peltier plates and a heat sink, where both regions are held at 1°C. The water vapor will re-condense in calibration column 2, and if the steady state flow rate measured in calibration column 2 is equal to that measured in advance in calibration column 1, there is no water condensation between the two calibration columns. These methods ensure a flow rate uncertainty of 0.56% of the flow rate setpoint, leading to a maximum test uncertainty of  $\pm 0.056$  mg/s at a 10 mg/s flow rate.

#### **E. Propellant Feed System Control and Live Monitoring**

The heaters in the MIST system are controlled using an on/off control system with a relay board to regulate power to the heaters. The heaters are divided into three different circuits, as shown in Fig. 2, where circuit 1 encompasses the in-line heater, circuit 2 covers all the heated lines outside the vacuum chamber, and circuit 3 regulates the heated lines inside the vacuum chamber. Each circuit uses a control thermocouple to provide the control system input. A user can control the setpoint temperature and monitor the pressure transducer and thermocouple data in the MIST system using a LabVIEW VI that communicates to the MIST system via MODBUS serial communication. The LabVIEW user interface is shown in Fig. 3.

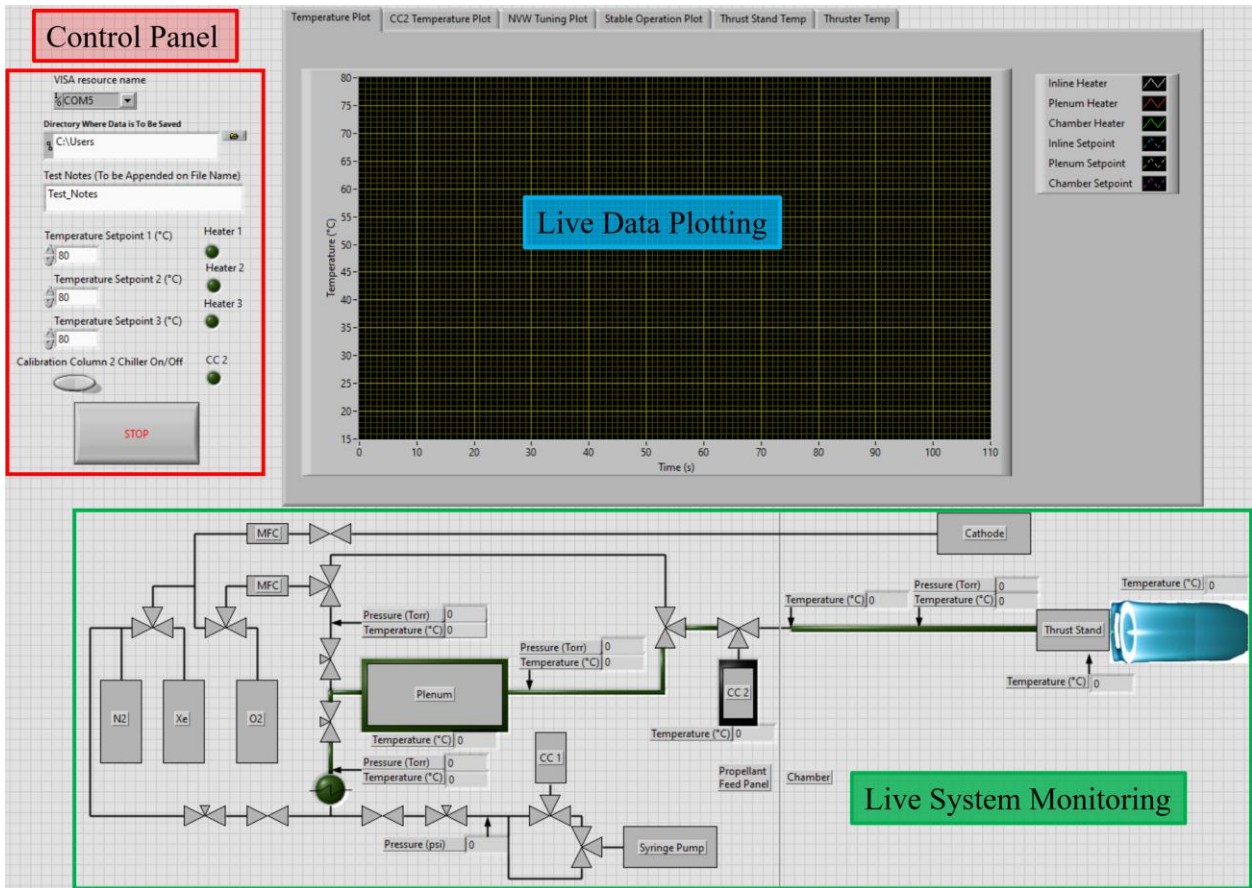


Figure 3. MIST system LabVIEW user interface.

The live data plotting capability allows the operator to determine when the propellant, particularly the water vapor component, is in a steady state prior to starting the thruster. The live system monitoring presents a holistic view of the MIST system, including pressures and temperatures throughout the system and when each heater is engaged. Data from all sensors are recorded and saved to a csv file.

#### IV. Propellant Feed System Validation

Once the MIST system was constructed, it underwent a series of validation tests to ensure nominal operation. The following subsections overview the validation tests, which include a leak check test, water condensation test, and thruster hot-fire test on a 5-kW HET.

##### A. Leak Check Verification Test

The first validation test sought to verify system adherence to high-level Requirement 7, which states that the leak rate of the system shall be less than 0.5 sccm on nitrogen at 30 psi. To perform this leak test, the authors disconnected the propellant line from the thruster and capped the end. The primary anode MFC was fed upstream with 30 psig nitrogen and pressurized the system until the system reached a pressure balance across the MFC. At this point, the MFC flow rate dropped to zero, indicating the system had no discernable leaks, and any remaining leakage in the MIST system was much less than 0.5 sccm. As a secondary test, the authors used leak detection fluid while the system was at pressure to ensure no visible leaks. These leak check tests validate Requirement 7.

##### B. Water Condensation Validation Test

The next validation test sought to verify system adherence to high-level Requirement 2 and the effective mitigation of Risk i to ensure water will not condense within the MIST system. As outlined in Section III.D., the water condensation test ensures water does not condense between the two calibration columns, as shown in the P&ID in Fig. 2. This region is the highest-pressure region in the MIST system, and the most likely region for water to condense.

Chilling calibration column 2 causes the water to re-condense, allowing for the effective measurement of the water vapor flow rate through this section. If the flow rate measured in calibration column 2 is lower than that supplied by the syringe pump and measured in calibration column 1, this indicates that water vapor mass is lost somewhere in the feed system by either a leak path or by condensation.

Water is the most likely to condense at the highest operating pressures, which will occur at the maximum designed flow rate condition of 10 mg/s. Due to this, a water condensation validation test at a 10 mg/s flow rate bounds the designed flow rate range. The condensation validation test occurred at flow rate steady state, seen with constant pressures among all pressure transducers, until the syringe pump delivered 10 mL of water. This occurred in 16.67 min at the 10 mg/s flow rate. Fig. 4 presents before and after results from the condensation validation test. As seen in the figure, 10 mL of water condensed in calibration column 2 in 16.67 min within 1% uncertainty, thus validating Requirement 2 and ensuring negligible condensation of water in the MIST system.

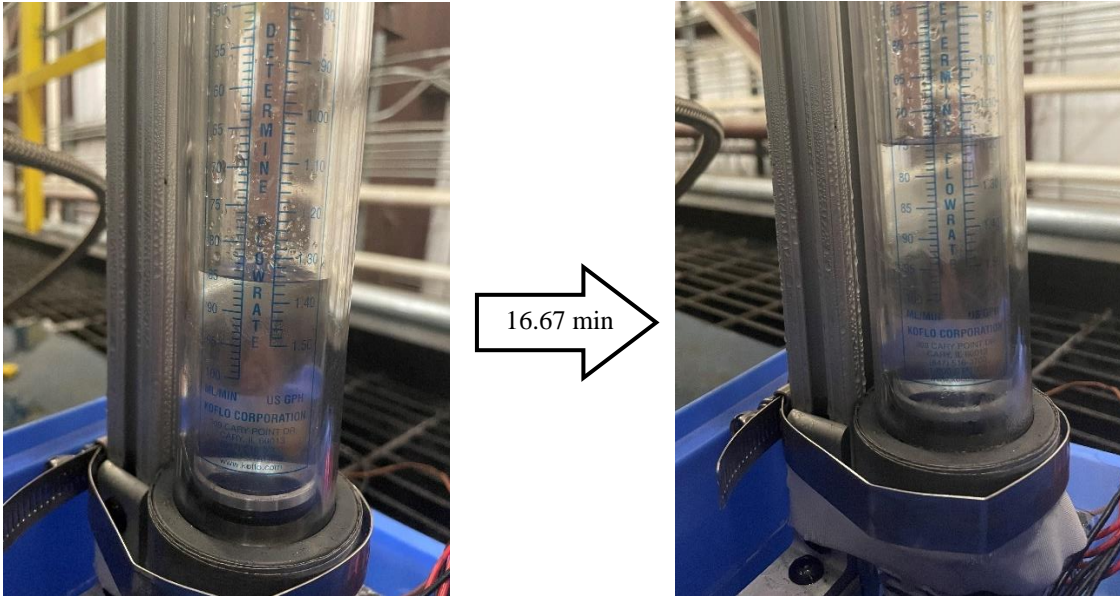


**Figure 4. Water condensation validation test on the MIST system using calibration column 2. The mass flow rate for this validation test is 10 mg/s.**

### C. Hot-Fire Test on a Hall Effect Thruster

The goal of the final validation test of the MIST system is to test the functionality of each operational mode during a hot-fire test on a laboratory HET. Specifically, this test sought to verify system adherence to Requirements 1 and 6 and ensure stable operation of the HET using the MIST system. The authors selected the P5 HET, which is a 5-kW laboratory thruster, to perform the hot-fire validation test. The P5 operated on xenon and nitrogen to verify operation in the pure gas mode, a krypton and argon mixture to verify operation in the gas mixture mode, and water vapor to verify operation in the water vapor mode. All setpoints from the hot-fire test are presented in Table 5. These setpoints capture the stable operating point of the P5 on each propellant.

**Table 5. Hot-fire HET operational setpoints.**

Setpoint	MIST Operational Mode	Anode Propellant	Cathode Propellant	Anode Flow Rate, (mg/s)	Cathode Flow Rate, (mg/s)	Discharge Voltage, (V)	Discharge Power, (kW)
1	Pure Gas	Xenon	Xenon	5.0	0.44	274	2.0
2	Pure Gas	Nitrogen	Xenon	5.0	0.44	279	4.3
3	Gas Mixture	Krypton/Argon	Krypton	3.1 (Kr) 1.4 (Ar)	0.41	236	2.6
4	Water Vapor	Water Vapor	Xenon	5.0	0.44	250	3.5

All testing was performed in Vacuum Test Facility 1 at Georgia Tech, and all operational chamber pressures were below  $5 \times 10^{-5}$  Torr, corrected for the respective propellant. The P5 operated for at least two consecutive hours at

each setpoint. Fig. 5 presents the P5 HET operating on each of the propellants supplied with the MIST system operating in its various propellant supply modes.

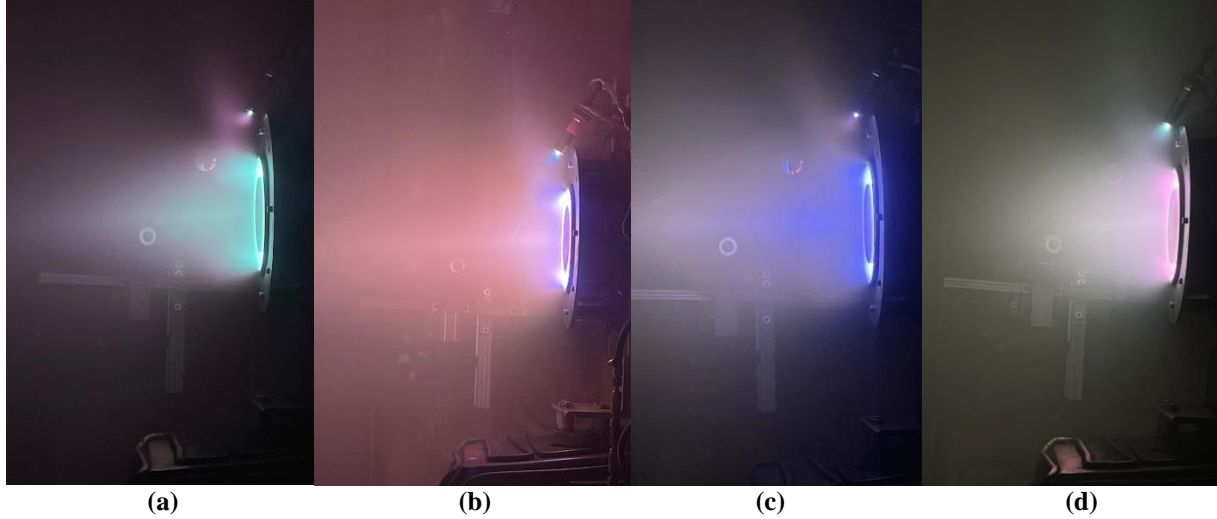


**Figure 5. P5 operating in pure gas mode (a)(b), gas mixture mode (c), and water vapor mode (d) using the MIST system. (a) has xenon through the anode and cathode, (b) has nitrogen through the anode and xenon through the cathode (b), (c) has a krypton/argon mixture through the anode and krypton through the cathode, and (d) has water vapor through the anode and xenon through the cathode.**

The P5 reached thermal and discharge stability, classified by a thruster body temperature variation less than 2 °C/hr and an average discharge current variation less than 1% over five minutes, running on each of the propellants in the hot-fire validation test. The successful thruster stability conditions using each of the MIST system operational modes validate Requirement 1. In the validation of Requirement 6, which ensures the peak-to-peak oscillations of the propellant flow rate remain under  $\pm 10\%$  deviation from the mean, the water vapor constituent demonstrated the largest oscillations. A sample start-up profile of the water vapor constituent, illustrating these oscillations, is shown in Fig. 6. In the figure, the pressure transducer directly upstream of the backpressure regulator records the liquid water pressure, and the pressure transducer directly downstream of the plenum captures the plenum pressure. The locations of these pressure transducers are shown in the P&ID in Fig. 2.

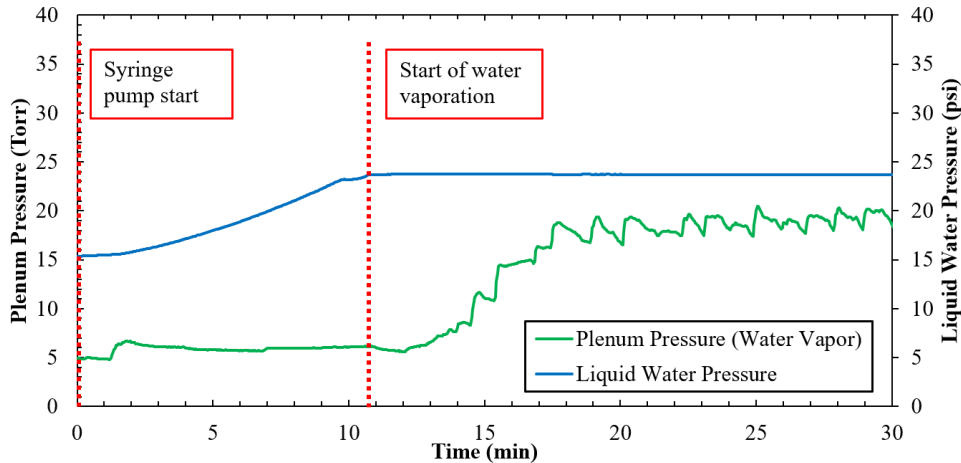


**Figure 6. MIST system water vapor start-up pressures.**

The flow rate of water vapor to the thruster scales by the square root of plenum pressure for a fixed anode cross section and water vapor temperature as mentioned in ISO 5167<sup>17</sup>. Thus, the resultant peak-to-peak oscillation in the water vapor flow rate is determined by analyzing the peak-to-peak oscillation in plenum pressure. The maximum measured peak-to-peak oscillation of the plenum pressure is  $\pm 8.6\%$ , which results in an approximate maximum peak-

to-peak oscillation of the delivered water vapor flow rate of  $\pm 4.2\%$ . This meets the stability requirement, thus validating Requirement 6. Additional plenum volume and operation at a higher water vapor mass flow rate can further mitigate these remaining water vapor oscillations.

## V. Conclusion

This paper overviews the design, calibration, and testing of the MIST system, which can supply a pure gas, pure gas mixture, or condensable vapor to an EP device. The current testing validates the MIST system to supply propellants in the pure gas, gas mixture, and condensable vapor modes at a mass flow rate of 0.5-10 mg/s, maximum uncertainty of 5%, and maximum peak-to-peak oscillation of  $\pm 10\%$  of the current flow rate setpoint. Many of the components in the MIST system are interchangeable to allow for alternative operating regimes, and these validation bounds can be adjusted with further testing.

The operation mode seen to produce the largest oscillations is the condensable gas mode, seen with approximate peak-to-peak flow rate oscillations of  $\pm 4.2\%$  while running on water vapor at a flow rate of 5 mg/s. These oscillations can be further mitigated in the future by increasing the plenum volume or adding additional flow-dampening hardware to the MIST system. While no air mixtures were generated using the MIST system at the time of this paper, this is a primary design focus of the system, and this application will be explored in the future using the gas mixture mode.

## Acknowledgments

This material is based upon work supported by the National Science Foundation Graduate Research Fellowship under Grant No. DGE-2039655. Any opinions, findings, and conclusions or recommendations expressed in this material are those of the authors and do not necessarily reflect the views of the National Science Foundation.

## References

- <sup>1</sup>Rovey, J. L., Lyne, C. T., Mundahl, A. J., Rasmont, N., Glascock, M. S., Wainwright, M. J., and Berg, S. P., "Review of Multimode Space Propulsion," *Progress in Aerospace Sciences*, Vol. 118, Oct. 2020.  
<https://doi.org/10.1016/j.paerosci.2020.100627>.
- <sup>2</sup>Little, B., and Jugroot, M., "Bimodal Propulsion System for Small Spacecraft: Design, Fabrication, and Performance Characterization," *Journal of Propulsion and Power*, Vol. 57, No. 4, 2020.  
<https://doi.org/10.2514/1.A34555>.
- <sup>3</sup>Koizumi, H., Inagaki, T., Kasagi, Y., Naoi, T., Hayashi, T., Funase, R., and Komurasaki, K., "Unified Propulsion System to Explore Near-Earth Asteroids by a 50 kg Spacecraft," 28<sup>th</sup> Annual AIAA/USU Conference on Small Satellites, Logan, UT, 2014.
- <sup>4</sup>Schwertheim, A. and Knoll, A., "In Situ Utilization of Water as a Propellant for a Next-Generation Plasma Propulsion System," *Journal of the British Interplanetary Society*, Vol. 72, No. 1, 2019, pp. 7-11.
- <sup>5</sup>Tejeda, J. M. and Knoll, A., "A Water Vapour Fuelled Hall Effect Thruster: Characterization and Comparison with Oxygen," *Acta Astronautica*, Vol. 211, Oct. 2023, pp. 702-715.  
<https://doi.org/10.1016/j.actaastro.2023.06.046>.
- <sup>6</sup>Schwertheim, A., Muir, C., Knoll, A., Ferreri, A., Sadler, J., Galdamez, C., and Staab D., "Experimentally Demonstrating the Feasibility of Water as a Multimode Electric-Chemical Propellant," 37<sup>th</sup> International Electric Propulsion Conference, Cambridge, MA, 2022.
- <sup>7</sup>Shirasu, K., Kuwabara, H., Matsuura, M., Koizumi, H., Nakagawa, Y., Watanabe, H., Sekine, H., and Komurasaki, K., "Demonstration and Experimental Characteristics of a Water-Vapor Hall Thruster," *Journal of Electric Propulsion*, Vol. 2, No. 11, 2023.  
<https://doi.org/10.1007/s44205-023-00047-w>.
- <sup>8</sup>Kotwicki, V., "Water in the Universe," *Hydrological Sciences Journal*, Vol. 36, No. 1, 1991, pp. 49-66.  
<https://doi.org/10.1080/02626669109492484>.
- <sup>9</sup>Hauer, I. M., Deblais, A., Beattie, J. K., Kellay, H., and Bonn, D., "The Dynamic Surface Tension of Water," *The Journal of Physical Chemistry Letters*, Vol. 8, No. 7, 2017, pp. 1599-1603.  
<https://doi.org/10.1021/acs.jpcclett.7b00267>.
- <sup>10</sup>Tirila, V., Demaire, A., and Ryan, C., "Review of Alternative Propellants in Hall Thrusters," *Acta Astronautica*, Vol. 212, Aug. 2023, pp. 284-306.  
<https://doi.org/10.1016/j.actaastro.2023.07.047>
- <sup>11</sup>Tisaev, M., Ferrato, E., Giannetti, V., Paissoni, C., Baresi, N., Lucca Fabris, A., and Andreussi, T., "Air-Breathing Electric Propulsion: Flight Envelope Identification and Development of Control for Long-Term Orbital Stability," *Acta Astronautica*, Vol. 191, Feb. 2022, pp. 374-393.  
<https://doi.org/10.1016/j.actaastro.2021.11.011>.
- <sup>12</sup>Crisp, N. H., Roberts, P. C. E., Livadiotti, S., Oiko, V. T. A., Edmondson, S., Haigh, S. J., Huyton, C., Sinpetru, L. A., Smith, K. L., Worrall, S. D., Becedas, J., Dominguez, R. M., Gonzalez, D., Hanessian, V., Molgaard, A., Nielsen, J., Bisgaard, M., Chan,

Y. A., Fasoulas, S., Herdrich, G. H., Romano, F., Traub, C., Garcia-Alminana, D., Rodrigues-Donaire, S., Sureda, M., Kataria, D., Outlaw, R., Belkouchi, B., Conte, A., Perez, J. S., Villain, R., Heiberer, B., and Schwalber, A., "The Benefits of Very Low Earth Orbit for Earth Observation Missions," *Progress in Aerospace Sciences*, Vol. 117, Aug. 2020.  
<https://doi.org/10.1016/j.paerosci.2020.100619>.

<sup>13</sup>"US Standard Atmosphere, 1976," National Oceanic and Atmospheric Administration, ADA035728, Washington, D.C., Oct. 1976.

<sup>14</sup>Gan, Q., Eastes, R. W., Wu, Y., Qian, L., Cai, X., Wang, W., England, S. L., and McClintock, W. E., "Thermospheric Responses to the 3 and 4 November 2021 Geomagnetic Storm During the Main and Recovery Phases as Observed by NASA's GOLD and ICON Missions," *Geophysical Research Letters*, Vol. 51, No. 1, 2024.  
<https://doi.org/10.1029/2023GL106529>.

<sup>15</sup>Hirshorn, S., Voss, L., and Bromley, L., "NASA Systems Engineering Handbook," NASA HQ-E-DAA-TN38707, Feb. 2017.

<sup>16</sup>"Design Considerations for Fluid Tubing Systems," NASA Preferred Reliability Practices No. PD-ED-1224.

<sup>17</sup>"Measurement of Fluid Flow by Means of Pressure Differential Devices Inserted in Circular Cross-Section Conduits Running Full," International Standard ISO 5167-1, 2003.

<sup>18</sup>Nakagawa, Y., Koizumi, H., Naito, Y., and Komurasaki, K., "Water and Xenon ECR Ion Thruster – Comparison in Global Model and Experiment," *Plasma Sources Science and Technology*, Vol. 29, Oct. 2020.  
<https://doi.org/10.1088/1361-6595/aba2ac>.

<sup>19</sup>Gallucci, S. E., Micci, M. M., and Bilen, S. G., "Design of a Water-Propellant 17.8-GHz Microwave Electrothermal Thruster," 35<sup>th</sup> International Electric Propulsion Conference, Atlanta, GA, 2017.

<sup>20</sup>Batliner, M., Weiss, M., Dual, S. A., Grass, B., Meboldt, M., and Daners, M. S., "Evaluation of a Novel Flow-Controlled Syringe Infusion Pump for Precise and Continuous Drug Delivery at Low Flow Rates: A Laboratory Study," *Anaesthesia*, Vol. 74, No. 11, 2019, pp. 1425-1431.  
<https://doi.org/10.1111/anae.14784>.

<sup>21</sup>Colangelo, A., Clark, S. T., and Janousek, J. P., "Implementation and Cost Analysis of a Syringe Pump System for Intermittent I.V. Drug Delivery," *American Journal of Hospital Pharmacy*, Vol. 42, Mar. 1985, pp. 581-584.

<sup>22</sup>Snyder, J. S., Baldwin, J., Frieman, J. D., Walker, M. L. R., Hicks, N. S., Polzin, K. A., Singleton, J. T., "Flow Control and Measurement in Electric Propulsion Systems: Towards an AIAA Reference Standard," 33<sup>rd</sup> International Electric Propulsion Conference, Washington D.C., 2013.